Fast Node Communication ADMM-based Imaging Algorithm with a Compressive Reflector Antenna

Juan Heredia-Juesas*†, Ali Molaei *, Luis Tirado*, Jose A. Martinez-Lorenzo*†
*Electrical and Computer Engineering (ECE). Northeastern University, Boston, MA, US.
†Mechanical and Industrial Engineering (MIE). Northeastern University, Boston, MA, US.
j.martinez-lorenzo@northeastern.edu

***Abstract*—This paper presents a norm-1 regularized algorithm, based on the Alternating Direction Method of Multipliers (ADMM), in which the sensing matrix is divided by columns. This technique is based on *sectioning* the imaging domain into different regions and optimizing them in distributed computational nodes. The information shared among nodes is highly reduced compared to the *consensus*-based ADMM, when dividing the matrix by rows. The combination of the *sectioning*-based ADMM with the imaging capabilities of the recently proposed Compressive Reflector Antenna allows a distributed, real-time imaging with fast node communication.**

I. Introduction

Compressive Reflector Antennas (CRAs) have been recently proposed as a way to enhance the sensing capacity of imaging systems [1], [2]. The use of CRAs relies on the use of Compressive Sensing (CS) techniques [2], [3]. This paper presents an imaging technique based on the Alternating Direction Method of Multipliers (ADMM) when dividing the sensing matrix in submatrices by columns. This leads to sectioning the image into regions and optimizing them in parallel, reducing the elements to be shared among nodes when comparing with the *consensus*-based ADMM technique [2]. The *sectioning*-based ADMM together with the CRA allows real-time imaging with fast node communication in a distributed scenario.

II. Compressive Reflector Antenna

The CRA is designed as described in [1], introducing discrete scatterers Ω_i on the surface of a Traditional Reflector Antenna (TRA). These scatterers generate a spatially coded radiation pattern that allow the use of CS techniques to generate a 3D image of an object under test. Some geometrical parameters are common for CRA and TRA: D, aperture size; f, focal length; h_o, offset height. Based on the configuration defined in Fig. 1, the coded pattern with N_{Tx} transmitter and N_{Rx} receiver horns is generated. Each receiver collects the signal from each transmitter for N_f frequencies, for a total of $N_m = N_{Tx} \cdot N_{Rx} \cdot N_f$ measurements. The image reconstruction domain is performed in N_p pixels, on a region of interest (ROI) located z_0^T away from the focal point of the CRA. The sensing matrix $\mathbf{H} \in \mathbb{C}^{N_m \times N_p}$, computed as described in [4], establishes a linear relationship between the unknown vector of reflectivity in each pixel $\mathbf{u} \in \mathbb{C}^{N_p}$, and the measured field data $\mathbf{g} \in \mathbb{C}^{N_m}$, which can be expressed in a matrix form, considering the noise $\mathbf{w} \in \mathbb{C}^{N_m}$, as follows:

$$\mathbf{g} = \mathbf{H}\mathbf{u} + \mathbf{w}. \tag{1}$$

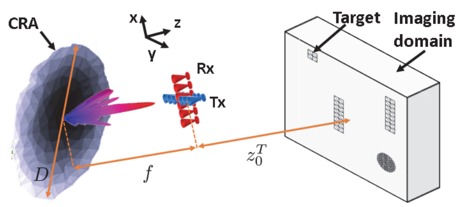

Fig. 1. Geometry of the sensing system, with the feed horns at the focal plane of the CRA.

III. Sectioning-based ADMM

A. Mathematical formulation

The ADMM [5] is a novel method for optimizing convex functions. Its general representation takes the following form:

$$\text{minimize } f(\mathbf{u}) + g(\mathbf{v}) \quad \text{s.t.} \quad \mathbf{P}\mathbf{u} + \mathbf{Q}\mathbf{v} = \mathbf{c} \tag{2}$$

Equation (1) may be solved by minimizing the convex function $f(\mathbf{u}) = \|\mathbf{H}\mathbf{u} - \mathbf{g}\|_2^2$ together with the norm-1 regularization $g(\mathbf{v}) = \lambda \|\mathbf{v}\|_1$. The proposed approach divides $\mathbf{H}$ into N submatrices $\mathbf{H}_j \in \mathbb{C}^{N_m \times \frac{N_p}{N}}$ and, consequently, the vector $\mathbf{u}$ into N subvectors $\mathbf{u}_j \in \mathbb{C}^{\frac{N_p}{N}}$. A new underdetermined problem $\sum_{j=1}^{N} \mathbf{H}_j \mathbf{u}_j = \mathbf{g}$ is optimized as follows:

$$\begin{aligned} \text{minimize} \quad & \frac{1}{2}\left\| \sum_{j=1}^{N} \mathbf{H}_j \mathbf{u}_j - \mathbf{g} \right\|_2^2 + \lambda \sum_{j=1}^{N} \|\mathbf{v}_j\|_1 \\ \text{s.t.} \quad & \mathbf{u}_j = \mathbf{v}_j, \quad \forall j = 1, ..., N. \end{aligned} \tag{3}$$

This problem is solved by the following iterative scheme:

$$\mathbf{u}_j^{(k+1)} = \left(\mathbf{H}_j^* \mathbf{H}_j + \rho \mathbf{I}_{\frac{N_p}{N}}\right)^{-1} \left(\mathbf{H}_j^* \mathbf{g}_j^{(k)} + \rho\left(\mathbf{v}_j^{(k)} - \mathbf{s}_j^{(k)}\right)\right), \tag{4}$$

$$\mathbf{v}_j^{(k+1)} = \mathbf{S}_{\frac{\lambda}{\rho}}\left(\mathbf{u}_j^{(k+1)} + \mathbf{s}_j^{(k)}\right), \tag{5}$$

$$\mathbf{s}_j^{(k+1)} = \mathbf{s}_j^{(k)} + \mathbf{u}_j^{(k+1)} - \mathbf{v}_j^{(k+1)}, \tag{6}$$

where $\mathbf{s}_j$ is the dual variable for each constraint j, ρ is the augmented parameter, $\mathbf{S}_\kappa(a)$ is the soft thresholding operator [6], and the vector $\mathbf{g}_j^{(k)}$ is defined as follows:

$$\mathbf{g}_j^{(k)} = \mathbf{g} - \sum_{q=1,\, q\neq j}^{N} \mathbf{H}_q \mathbf{u}_q^{(k)} = \mathbf{g} - \sum_{q=1,\, q\neq j}^{N} \hat{\mathbf{g}}_q^{(k)}, \tag{7}$$

If $N_m < \frac{N_p}{N}$, the *matrix inversion lemma* [7] can be applied to the term $\left(\mathbf{H}_j^* \mathbf{H}_j + \rho \mathbf{I}_{\frac{N_p}{N}}\right)^{-1}$, since only N matrices of sizes $N_m \times N_m$ would need to be inverted.

B. Communication among nodes

The *sectioning*-based ADMM technique may be seen as N fully-connected nodes that have the information of each submatrix $\mathbf{H}_j$ and the vector of measurements $\mathbf{g}$. Each node optimizes each subvector $\mathbf{u}_j$ and share their particular solution with the remaining nodes in the format $\hat{\mathbf{g}}_j = \mathbf{H}_j \mathbf{u}_j$. Therefore, small vectors need to be shared. At iteration k, each node j receives $N-1$ vectors $\hat{\mathbf{g}}_q^{(k)} \in \mathbb{C}^{N_m}$, $(q \neq j)$ and transmits the vector $\hat{\mathbf{g}}_j^{(k)} \in \mathbb{C}^{N_m}$, as represented in Fig. 2(a). Therefore, $N \cdot N_m$ elements are transmitted. In the case of the *consensus*-based ADMM technique [2], the whole vector $\mathbf{v}^{(k)} \in \mathbb{C}^{N_p}$ is received and the new update $\mathbf{u}^{i(k+1)} \in \mathbb{C}^{N_p}$ is transmitted from the node i at each iteration, as Fig. 2(b) shows, so $2N_p$ elements need to be transmitted. In conclusion, the technique of dividing $\mathbf{H}$ by columns is more efficient than dividing $\mathbf{H}$ by rows, when the inequation $N \cdot N_m < 2N_p$ is satisfied.

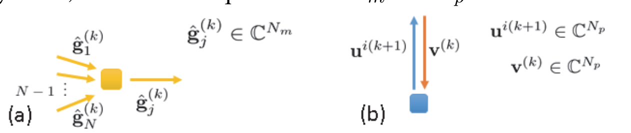

Fig. 2. Communication vectors in a single node for one iteration when the sensing matrix is divided (a) by columns, (b) by rows.

IV. Numerical Results

The performance of this technique is evaluated by the use of a CRA via a mm-wave imaging application. Each scatterer Ω_i is considered as a perfect electric conductor. The CRA is discretized into triangular patches, as described in [4], characterized by an averaged size of $\langle D^x \rangle$ and $\langle D^y \rangle$. The scatterer size D_i^z is computed as $\langle D^x \rangle \cdot \tan(\alpha_t)$, where α_t is the tilt angle, modeled as a uniform random variable in the interval $[0, \alpha_{tmax}]$. λ_c is the wavelength at the center frequency f_c. The ROI encloses a volume determined by Δx_0^T, Δy_0^T, and Δz_0^T; and it is discretized into parallelepipeds of side length l_x, l_y, and l_z. The parameters for the numerical simulation are shown in Table I.

TABLE I
Parameters for the numerical example.

Param.	Value	Param.	Value	Param.	Value
f_c	73.5 GHz	$\langle D^y \rangle$	$10\lambda_c$	z_0^T	$195\lambda_c$
BW	7 GHz	α_{tmax}	$5°$	Δx_0^T	$54\lambda_c$
λ_c	$4.1cm$	N_{Tx}	6	Δy_0^T	$54\lambda_c$
D	$61\lambda_c$	N_{Rx}	6	Δz_0^T	$7.5\lambda_c$
f	$122\lambda_c$	N_f	12	l_x	$1.08\lambda_c$
h_o	$0\lambda_c$	N_m	432	l_y	$1.08\lambda_c$
$\langle D^x \rangle$	$10\lambda_c$	N_p	$30,000$	l_z	$1.25\lambda_c$

For this example, the sensing matrix $\mathbf{H}$ has a size of $N_m \times N_p = 432 \times 30000$. The proposed technique divides $\mathbf{H}$ into $N = 4$ columns of size 432×7500. Figure 3 shows the imaging results applying the *sectioning*-based ADMM technique, with a norm-1 weight of $\lambda = 1000$ and an augmented parameter of $\rho = 5$, for a structure of four targets located among six parallel planes. This algorithm performs the imaging in $1.0s$ for 45 iterations in a MATLAB 2017b PCT M code, using a NVIDIA Quadro P6000, 3840 cores GPU, with single precision computation.

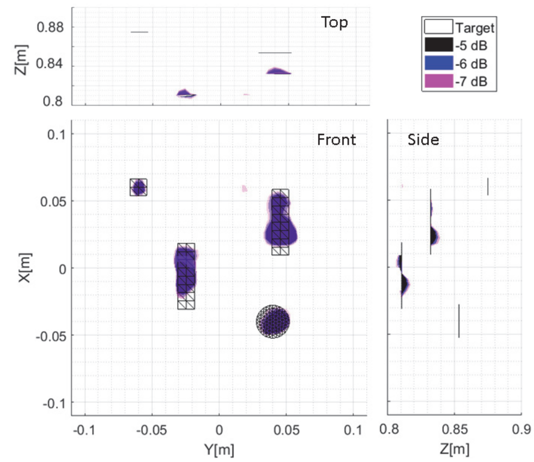

Fig. 3. Imaging reconstruction (top, front, and side views) with ADMM dividing by columns. The targets are represented with the transparent triangles and the normalized reconstructed reflectivity is presented in the colored map.

In terms of communication among nodes, the technique of dividing the sensing matrix in four submatrices by columns is more efficient than the technique of dividing the matrix by rows, since $N \cdot N_m = 1728 < 60,000 = 2 \cdot N_p$, reducing the elements to be shared for one node by 97.1%.

V. Conclusion

This paper has presented the mathematical formulation of a new distributed imaging algorithm based on the norm-1 regularized ADMM when dividing the sensing matrix by columns. This technique has been tested by the use of a CRA. The distributive capabilities of the *sectioning*-based ADMM and fast communication among nodes, together with the high sensing capacity of the CRA, enable a real-time imaging.

ACKNOWLEDGEMENT

This work has been partially funded by the NSF CAREER program (Award No. 1653671), the Department of Energy (Award No. DE-SC0017614), and the U.S. Department of Homeland Security (Award No. 2013-ST-061-ED0001).

References

[1] J. Martinez Lorenzo, J. Heredia Juesas, and W. Blackwell, “A single-transceiver compressive reflector antenna for high-sensing-capacity imaging,” *IEEE Antennas and Wireless Propagation Letters*, vol. 15, pp. 968–971, March 2016.

[2] J. Heredia-Juesas, A. Molaei, L. Tirado, W. Blackwell, and J. Á. Martínez-Lorenzo, “Norm-1 regularized consensus-based admm for imaging with a compressive antenna,” *IEEE Antennas and Wireless Propagation Letters*, vol. 16, pp. 2362–2365, 2017.

[3] S. Becker, J. Bobin, and E. J. Candès, “Nesta: a fast and accurate first-order method for sparse recovery,” *SIAM Journal on Imaging Sciences*, vol. 4, no. 1, pp. 1–39, 2011.

[4] J. Meana, J. Martinez-Lorenzo, F. Las-Heras, and C. Rappaport, “Wave scattering by dielectric and lossy materials using the modified equivalent current approximation (meca),” *Antennas and Propagation, IEEE Transactions on*, vol. 58, no. 11, pp. 3757–3761, Nov 2010.

[5] S. Boyd and L. Vandenberghe, *Convex optimization*. Cambridge university press, 2009.

[6] D. L. Donoho, “De-noising by soft-thresholding,” *IEEE transactions on information theory*, vol. 41, no. 3, pp. 613–627, 1995.

[7] M. A. Woodbury, “Inverting modified matrices,” *Memorandum report*, vol. 42, p. 106, 1950.